



Article

Impact of Amyloid- β on Platelet Mitochondrial Function and Platelet-Mediated Amyloid Aggregation in Alzheimer's Disease

Lili Donner ^{1,*}, Tobias Feige ¹, Carolin Freiburg ¹, Laura Mara Toska ¹, Andreas S. Reichert ² ,
Madhumita Chatterjee ³ and Margitta Elvers ^{1,*}

¹ Department of Vascular and Endovascular Surgery, Experimental Vascular Medicine, Medical Faculty and University Hospital Düsseldorf, Heinrich-Heine University Düsseldorf, 40225 Düsseldorf, Germany; Tobias.Feige@med.uni-duesseldorf.de (T.F.); Carolin.Freiburg@uni-duesseldorf.de (C.F.); LauraMara.Toska@med.uni-duesseldorf.de (L.M.T.)

² Institute of Biochemistry and Molecular Biology I, Medical Faculty and University Hospital Düsseldorf, Heinrich-Heine University Düsseldorf, 40225 Düsseldorf, Germany; reichert@hhu.de

³ Department of Cardiology and Angiology, Universitätsklinikum Tübingen, Medizinische Klinik III, 72076 Tübingen, Germany; madhumita.chatterjee@med.uni-tuebingen.de

* Correspondence: Lili.Donner@med.uni-duesseldorf.de (L.D.); Margitta.Elvers@med.uni-duesseldorf.de (M.E.)



Citation: Donner, L.; Feige, T.; Freiburg, C.; Toska, L.M.; Reichert, A.S.; Chatterjee, M.; Elvers, M. Impact of Amyloid- β on Platelet Mitochondrial Function and Platelet-Mediated Amyloid Aggregation in Alzheimer's Disease. *Int. J. Mol. Sci.* **2021**, *22*, 9633. <https://doi.org/10.3390/ijms22179633>

Academic Editor: Isabella Russo

Received: 20 July 2021

Accepted: 2 September 2021

Published: 6 September 2021

Publisher's Note: MDPI stays neutral with regard to jurisdictional claims in published maps and institutional affiliations.



Copyright: © 2021 by the authors. Licensee MDPI, Basel, Switzerland. This article is an open access article distributed under the terms and conditions of the Creative Commons Attribution (CC BY) license (<https://creativecommons.org/licenses/by/4.0/>).

Abstract: Background: Alzheimer's disease (AD) is characterized by an accumulation of amyloid β (A β) peptides in the brain and mitochondrial dysfunction. Platelet activation is enhanced in AD and platelets contribute to AD pathology by their ability to facilitate soluble A β to form A β aggregates. Thus, anti-platelet therapy reduces the formation of cerebral amyloid angiopathy in AD transgenic mice. Platelet mitochondrial dysfunction plays a regulatory role in thrombotic response, but its significance in AD is unknown and explored herein. Methods: The effects of A β -mediated mitochondrial dysfunction in platelets were investigated in vitro. Results: A β 40 stimulation of human platelets led to elevated reactive oxygen species (ROS) and superoxide production, while reduced mitochondrial membrane potential and oxygen consumption rate. Enhanced mitochondrial dysfunction triggered platelet-mediated A β 40 aggregate formation through GPVI-mediated ROS production, leading to enhanced integrin α IIb β 3 activation during synergistic stimulation from ADP and A β 40. A β 40 aggregate formation of human and murine (APP23) platelets were comparable to controls and could be reduced by the antioxidant vitamin C. Conclusions: Mitochondrial dysfunction contributes to platelet-mediated A β aggregate formation and might be a promising target to limit platelet activation exaggerated pathological manifestations in AD.

Keywords: Alzheimer's disease; platelets; mitochondria dysfunction; A β aggregation; cerebral amyloid angiopathy; ROS; GPVI; integrin

1. Introduction

The most prevalent form of dementia is Alzheimer's disease (AD). AD is characterized by the pathological hallmarks of abnormal accumulation of amyloid β (A β) peptides in the brain [1]. One of the earliest pathological alterations in AD is the dysfunction of mitochondria [2]. Mitochondrial abnormalities, such as impaired mitochondrial dynamics (increased fission and reduced fusion), altered morphology and mitochondrial gene expression, increased free radical production and lipid peroxidation, reduced cytochrome c oxidase (COX) activity and ATP production, are typical characteristics of AD. Mitochondrial dysfunction results from these morphological and metabolic alterations during the progression of AD [2–5]. Soluble A β enters mitochondria and is responsible for mitochondrial dysfunction that contributes to phosphorylation of tau, increased formation of free radicals, mtDNA damage and interaction of A β with Drp1, A β -binding alcohol dehydrogenase (ABAD) and cyclophilin D (CypD), loss of cytochrome c oxidase (COX) activity, impaired gating of the mitochondrial permeability transition pore and loss of membrane potential.

In the presence of A β , mitochondria are reduced in size due to excessive mitochondrial fragmentation and reduced mitochondrial fusion, but increased in numbers [6–10]. Increased levels of A β in the cytoplasm of AD neurons also lead to reduced levels of parkin and PTEN-induced putative kinase1 (PINK1) leading to the inability to clear damaged mitochondria (mitophagy) and other cellular debris from neurons [11]. Persisting mitochondrial dysfunction contributes to synaptic dysfunction because declined mitochondrial biogenesis leads to reduced ATP levels that is essential for delivery of neurotransmitters by synaptic vesicles to the synapse [12]. Furthermore, the loss of COX activates apoptotic pathways, leading to the loss of neurons in the central nervous system [6]. As a compensatory mechanism for dysfunctional energy metabolism, mitochondrial-encoded genes are upregulated in AD transgenic mice [10]. While mitochondrial dysfunction plays a central role in the pathogenesis of AD, the dysregulated mitophagy is causative in worsening disease pathology/severity in AD.

Platelets expose amyloid precursor protein (APP) at the platelet membrane and include all the necessary enzymes for the generation of different A β peptides from APP in their alpha granules [13]. Therefore, platelets are a source of A β peptides in blood [14]. Furthermore, apoptotic platelets are able to incorporate oligomeric A β 40 [15]. Different studies have identified pathological alterations in isolated platelets from AD patients, such as a decreased amyloid protein precursor ratio and an increased activity of β -secretase leading to A β production [16,17]. Moreover, AD patients exhibit increased basal activation of platelets, denoted by enhanced surface expression of P-selectin and presence of activated integrin $\alpha_{IIb}\beta_3$ [18]. Pre-activated platelets in the circulation are also observed in the AD transgenic mouse model APP23. These platelets adhere to amyloid deposits in cerebral vessels causing vessel occlusion [19]. A subpopulation of coated platelets with high procoagulant activity is elevated in AD patients and correlates with the progression of AD [20]. Interestingly, apart from their ability to generate A β peptides, predominantly A β 40, platelets also modify soluble synthetic A β 40 into toxic A β aggregates in vitro [15]. Platelet-specific receptors, namely integrin $\alpha_{IIb}\beta_3$ and collagen receptor glycoprotein (GP)VI, were identified as direct binding partners of A β 40 at the platelet membrane that contribute to platelet activation and aggregation of A β 40 peptides [21–23].

Although platelets contain only five to eight mitochondria per cell [24], they play an important role in energy metabolism and ATP production in platelets. Moreover, mitochondria are also involved in platelet activation and apoptosis [25]. Previous studies have provided evidence for altered mitochondrial function in platelets from AD patients. Compared to platelet mitochondria from healthy volunteers, platelet mitochondria from AD patients exhibit decreased maximal capacity of the electron transport system and reduced respiration rates [26,27]. In addition, platelets from AD patients show decreased COX activity, which is associated with ROS overproduction [28].

Despite the extensive research work in the last decades and the progress that has been made to understand the pathophysiology of AD, there are many open questions in understanding the molecular basis of the disease. However, it is well accepted that AD is a multi-factorial neurodegenerative disease and there is still no drug or therapy available to delay or even prevent dementia in patients with AD. In recent years it has been increasingly recognized that platelets can not only serve as a biomarker for the disease but also substantially contribute to the progression of AD. However, the impact of platelets in AD progression is not fully understood. Therefore, the present study aimed to investigate the effect of A β 40 peptides on platelet mitochondrial dynamics and its consequences for platelet activation and A β 40 aggregate formation.

2. Results

2.1. Effects of A β 40 on Mitochondria in Platelets

Generation of reactive oxygen species (ROS) plays an influential role in pathophysiological platelet functions [29]. To investigate the effect of A β 40 on intracellular ROS production in platelets, we measured ROS by flow cytometry using the dye DCF-DA.

The cellular ROS level in platelets from healthy donors was significantly increased upon stimulation with A β 40 (Figure 1A). In contrast, the stimulation with A β 1-16 (A β 16, used as negative control) did not lead to increased ROS levels. To determine the impact of A β 40 on mitochondrial superoxide production, we used the mitochondrial localized ROS sensitive dye MitoSOX-Red. The generation of mitochondrial superoxide was increased upon A β 40 stimulation and unaltered by A β 16 (Figure 1B). Using the cationic dye TMRM, we determined whether or not stimulation of platelets with A β 40 led to a loss of the mitochondrial transmembrane potential ($\Delta\psi_m$) (Figure 1C). As shown in Figure 1C, the incubation of platelets with A β 40 led to significantly reduced $\Delta\psi_m$ in platelets, whereas A β 16 showed no effect.

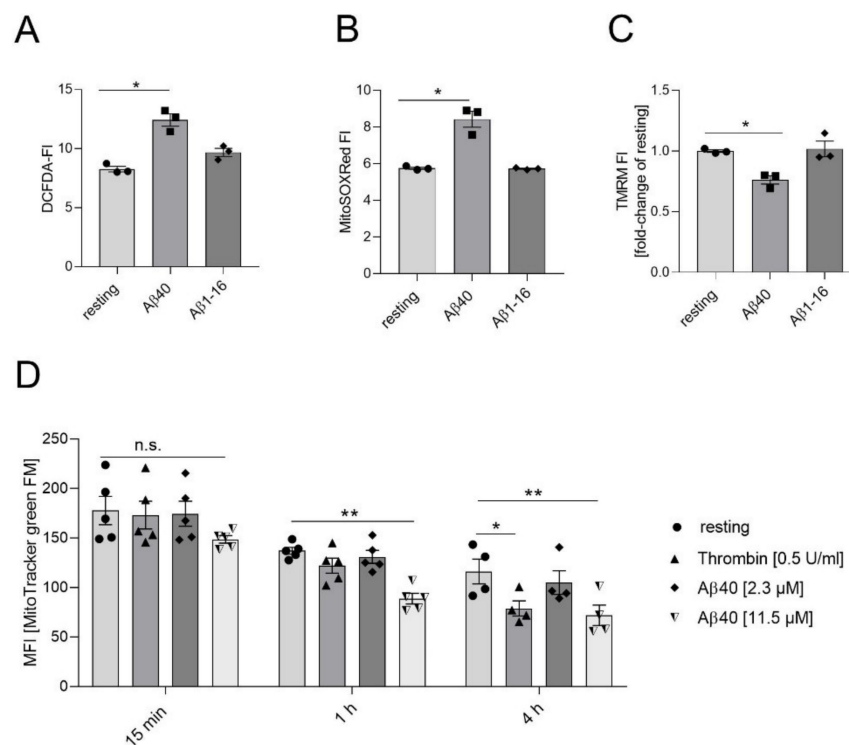


Figure 1. Impact of A β on mitochondrial functions in platelets. (A) Washed human platelets were incubated for 24 h with 11.5 μ M A β 40 and 11.5 μ M A β 1-16 (as control). Generation of ROS was reported as mean fluorescence intensity of DCF (n = 3). (B) MitoSOXRedTM-loaded platelets were incubated with 5 μ M A β 40 and 5 μ M A β 1-16 for 30 min and the generation of superoxide was measured as mean fluorescence intensity (n = 3). (C) Depolarization of the platelet mitochondrial membrane upon 5 μ M A β 40 and 5 μ M A β 1-16 was observed by decreased TMRM fluorescence intensity (n = 3). (D) The mitochondrial dye, MitoTrackerTM green FM, was added to platelets to determine the release of mitochondria upon A β 40 stimulation (n = 4–5). Compared to control (resting). (A–D) All samples were measured by flow cytometry. Bar graphs depict mean values \pm SEM. All analyses were performed using one-way ANOVA and Dunnett’s multiple comparisons post-hoc test. ** $p < 0.01$; * $p < 0.05$. n.s.: not significant.

Bourdeau and colleges have shown that activation of platelets induces release of mitochondria to promote inflammatory response [30]. Using a mitochondria-selective, yet membrane potential insensitive, fluorescent dye (MitoTrackerTM green FM, Invitrogen), we detected that thrombin activation of platelets led to a reduced mean fluorescence intensity (MFI) consistent with the release of mitochondria after 4 h of incubation (Figure 1D). By contrast, platelets started to release mitochondria upon stimulation with 11.5 μ M A β 40 already after 1 h and continued till 4 h of incubation, while no effects could be seen with lower concentrations of A β 40 (2.3 μ M) (Figure 1D).

2.2. Reduced Mitochondrial Respiration in Platelets Following A β 40 Treatment

Using the Seahorse Extracellular Flux Analyzer, platelet mitochondrial respiration was investigated after incubation with soluble A β 40 by measuring the oxygen consumption rate (OCR). A β 40 or vehicle (medium) was added to platelets for 30 min before measurement. The basal OCR in platelets in the presence of A β 40 was comparable to resting platelets (control) after 30 min (Figure 2A,B). After injection of collagen related peptide (CRP) to activate the major collagen receptor GPVI, we found a general stimulation of respiration rates (Figure 2A,C). Importantly, a significant relative reduction of OCR in platelets was evident always when A β 40 was added irrespective of the addition of CRP. A significant reduction of the OCR over time was also found when platelets were incubated with A β 40 compared to unstimulated platelets (Figure 2A,C). To measure ATP-linked respiration, the ATP synthase inhibitor oligomycin was added subsequently. Again, CRP induced an enhanced OCR compared to non-stimulated platelets. However, in the presence of A β 40, CRP-induced OCR was significantly reduced (Figure 2A,D). Afterwards, the proton ionophore and uncoupler FCCP was injected to measure maximal respiration (Figure 2A,E). As expected, the injection of FCCP led to increased respiration in CRP-stimulated platelets. Again, the presence of A β 40 reduced maximal respiration in both resting and in CRP-stimulated platelets. Moreover, the increase of CRP-induced maximal respiration was reduced to basal (resting) levels when platelets were incubated with A β 40 (Figure 2A,E). Proton leak across the inner mitochondrial membrane was not changed in the presence of A β 40 (Figure 2A,F). Non-mitochondrial respiration ascertained using the mitochondrial complex inhibitors Antimycin A and Rotenone was not altered between groups (Figure 2A,G). Taken together, these results demonstrate that A β 40 negatively impacts mitochondrial respiration in resting and CRP-stimulated platelets.

2.3. Impact of Extracellular A β 40 on Mitochondrial Proteins

To investigate the impact of extracellular A β 40 on mitochondrial proteins, such as PTEN-induced putative kinase 1 (PINK1), translocase of the inner membrane 23 (TIM23), 60 kDa heat shock protein (Hsp60), optic atrophy-1 (OPA1) and translocase of the outer membrane 20 (TOM20) in platelets, we incubated platelets with different concentrations of A β 40 for 2 h and analyzed protein expression by Western blot. Non-stimulated platelets were used as negative and CRP-stimulated platelets were used as positive control. The incubation with different concentrations of A β 40 for 1 h did not induce alterations in the level of the examined proteins (Figure S1). After incubation of platelets with A β 40 for 2 h, the protein levels of PINK1, TIM23 and Hsp60 were comparable to that of resting platelets (Figure 3A and Figure S2). However, the protein level of TOM20 was significantly reduced when human platelets were stimulated with intermediate and high concentrations of A β 40 as well as with CRP (Figure 3A,B), suggesting that downregulation of TOM20 is not due to A β 40 toxicity but due to platelet stimulation. Determination of the ratio of long OPA1/short OPA1 revealed no significant alterations and a trend towards a reduced ratio was only observed when platelets were stimulated with CRP. Addition of A β 40 did not significantly alter the ratio of long OPA1/short OPA1.

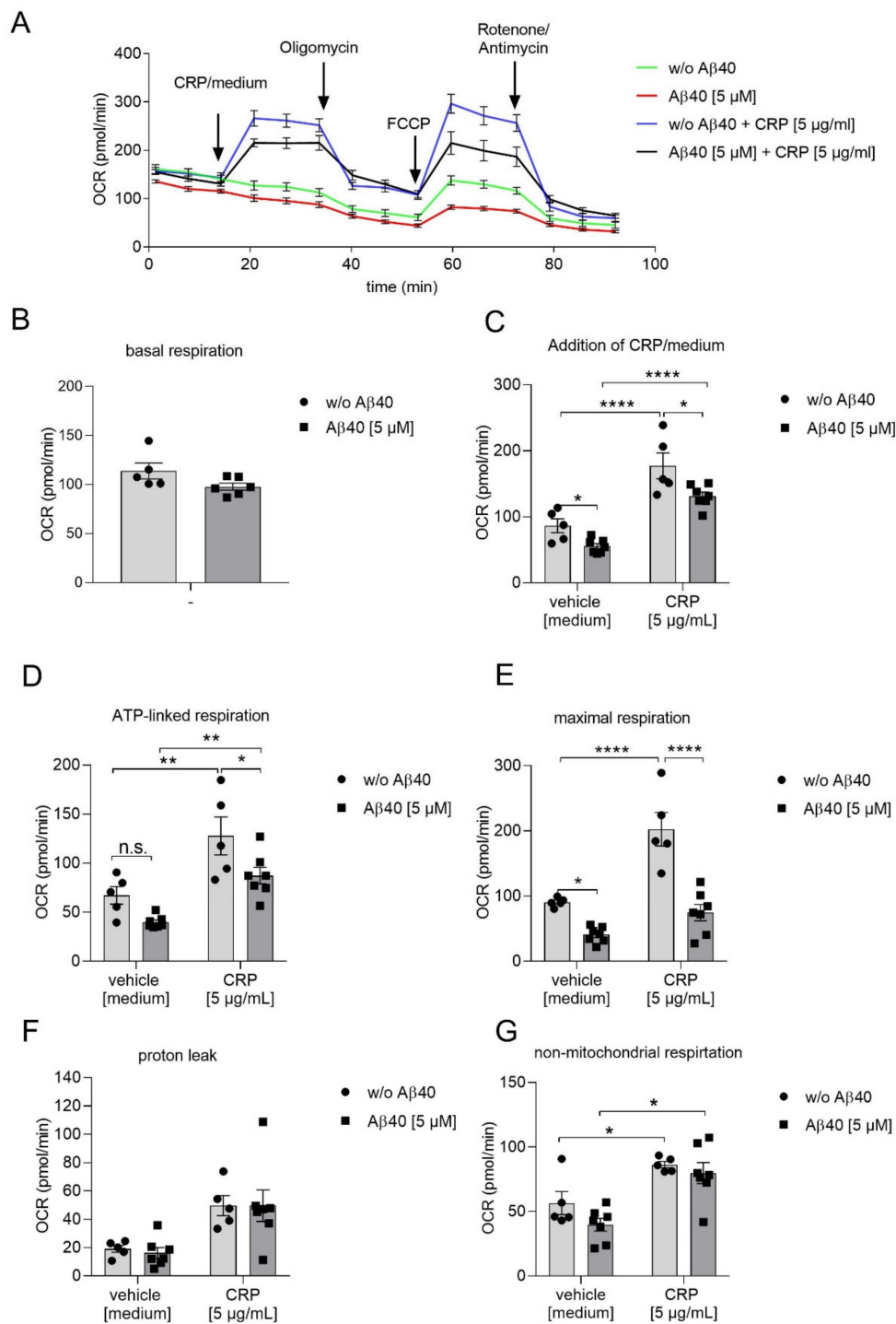


Figure 2. Determination of oxygen consumption rate (OCR) in human platelets upon treatment with Aβ40. (A) Determination of the oxygen consumption rate (OCR) after injection of indicated chemicals at indicated time points using a Seahorse XF24 analyzer. (B) Basal respiration, (C) respiration after addition of collagen-related peptide (CRP) or vehicle (medium), (D) ATP-linked respiration, (E) maximal respiration, (F) proton leak and (G) non-mitochondrial respiration. (A–G) Data represent mean ± SEM from n = 5–7 donors, two-way ANOVA with Holm-Sidak’s multiple comparisons test, **** = $p < 0.0001$; ** = $p < 0.01$; * = $p < 0.05$. w/o: Without; n.s.: Not significant.

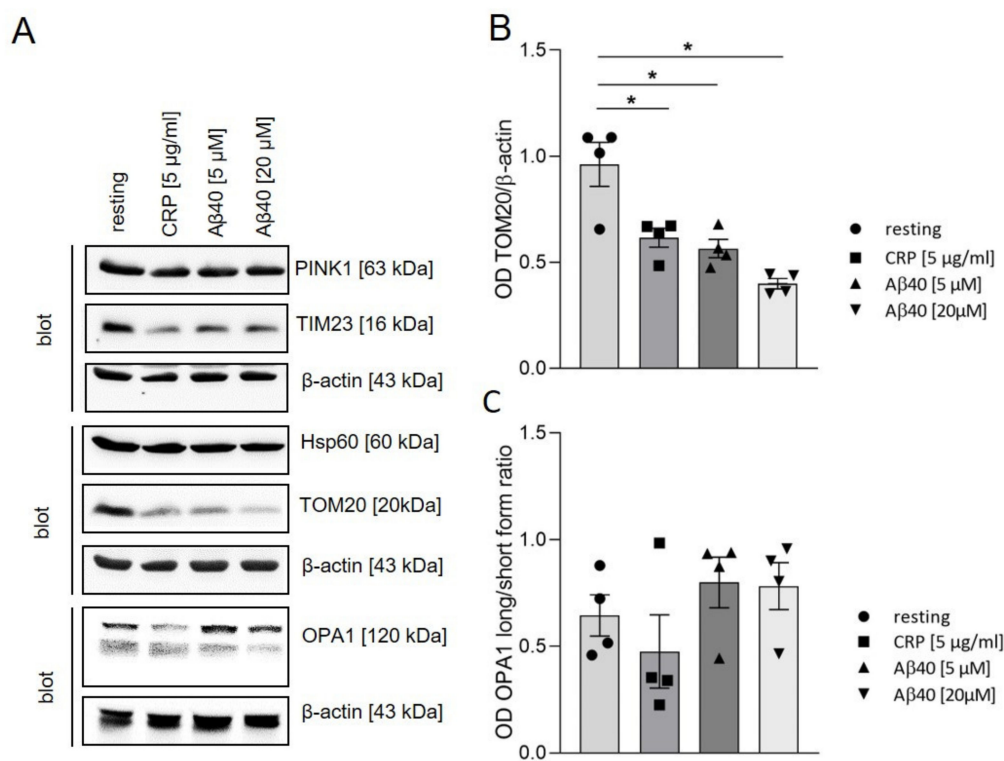


Figure 3. Expression levels of mitochondrial proteins in platelets upon A β 40 stimulation. (A) Human platelets were stimulated with 5 or 20 μ M A β 40 or 5 μ g/mL CRP for 2 h. Using Western blot analysis, the expression levels of mitochondrial proteins were detected as indicated. β -actin served as loading control. (B,C) The intensity of bands was analyzed with ImageJ software. Data represent mean value \pm SEM (n = 4). All analyses were performed using one-way ANOVA and Dunnett's multiple comparisons post-hoc test. * = $p < 0.05$.

2.4. Inhibition of Complex III Leads to Enhanced Platelet Mediated A β Aggregate Formation In Vitro

Platelets are able to modulate soluble, synthetic A β 40 into forming amyloid aggregates in vitro [15,21–23]. To analyze the role of mitochondria in platelet-mediated A β aggregation, we treated human platelets with antimycin A (or with EtOH as vehicle) and incubated the cells with soluble, synthetic A β 40 for three days. Treatment of platelets with synthetic A β 40 in presence of antimycin A led to increased A β aggregate formation in a concentration-dependent manner (Figure 4A,B). The highest aggregate formation was detected in the presence of 500 and 1000 ng/mL antimycin A. Previously it was demonstrated that complex III-derived ROS triggers the formation of A β by enhanced amyloidogenic amyloid precursor protein processing in HEK293 cells [31]. To investigate whether or not the inhibition of complex III per se leads to the production of A β 40 in platelets, we incubated platelets with antimycin A for 24 h. However, as shown in Figure 4C, no increase was detected in A β 40 levels after inhibition of the mitochondrial respiratory complex III (Figure 4C), suggesting that endogenous A β 40 production does not significantly contribute to A β 40 aggregate formation in platelet culture.

A β 40 induces ROS generation in platelets as shown in Figure 1A. To investigate whether or not elevated ROS levels play a role in platelet-mediated A β aggregation, we used the antioxidant vitamin C as ROS scavenger. The presence of vitamin C led to decreased amyloid aggregate formation in platelet cell culture (Figure 4D). To confirm this result, we quantified the remaining soluble A β 40 in the supernatants of platelet cell culture using Western blot analysis. The remaining amount of A β 40 was increased when platelets were incubated with vitamin C suggesting that ROS generation plays a crucial role in platelet-mediated A β aggregation (Figure 4E).

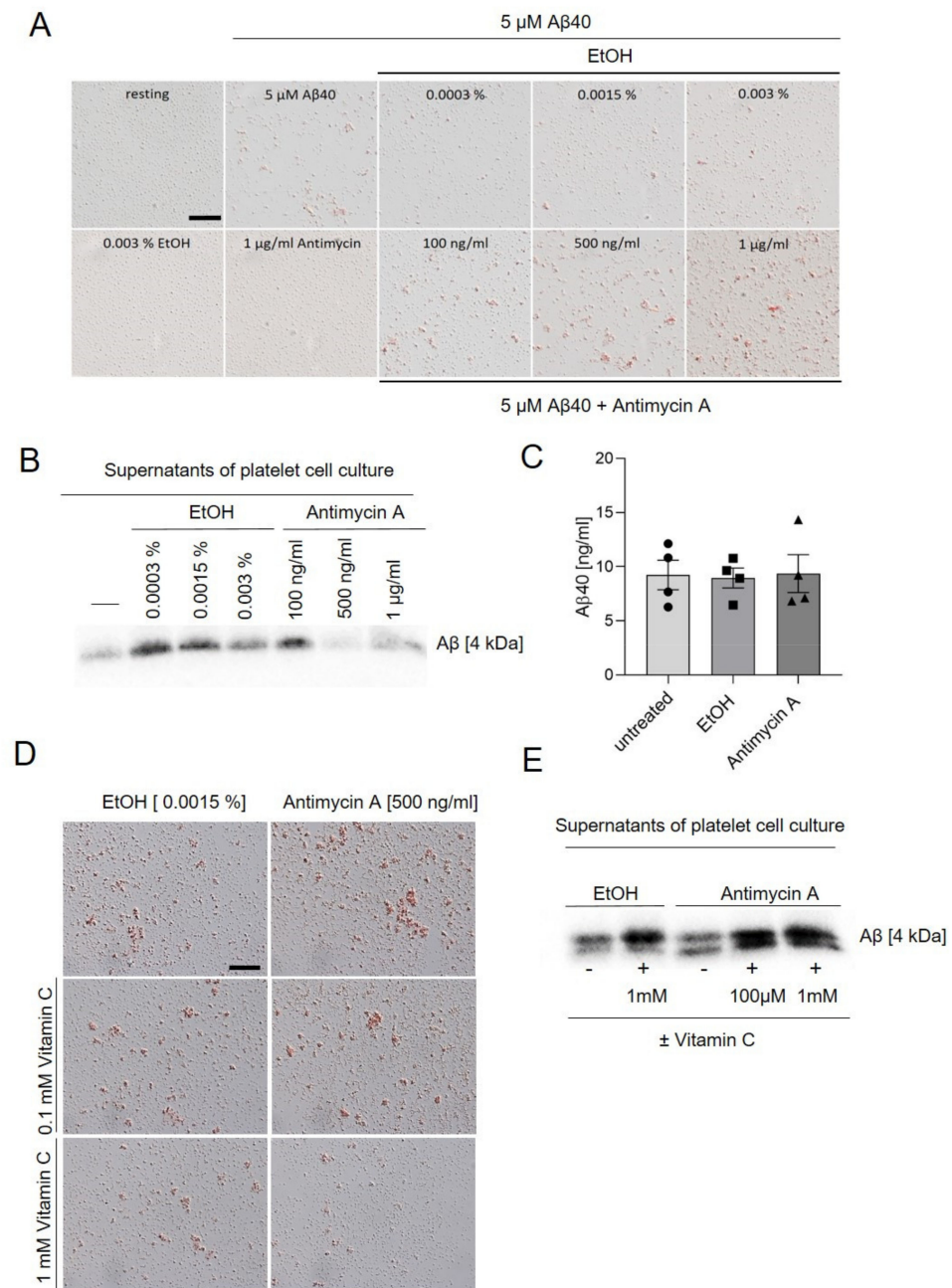


Figure 4. Effects of antimycin A and the antioxidant vitamin C on platelet-mediated A β aggregate formation. **(A)** Representative images of congo red-stained A β deposits in platelet culture. Platelets were incubated with 5 μ M of soluble synthetic A β 40 and different concentrations of antimycin A for three days at 37 $^{\circ}$ C and 5% CO $_2$. EtOH served as the control (vehicle). Scale bar, 50 μ m. **(B)** Quantification of remaining soluble A β 40 in the supernatant of platelet culture using Western blot. **(C)** Isolated platelets were incubated in the absence or presence of antimycin A (500 ng/mL) for 24 h at 37 $^{\circ}$ C. EtOH (0.0015%) served as solvent control for antimycin A. A β 40 levels were determined using ELISA (n = 4). **(D)** Platelet culture after incubation with soluble, synthetic A β 40 for three days. Where indicated, platelets were incubated with antimycin A (500 ng/mL) or antimycin A (500 ng/mL) and different concentrations of vitamin C (100 μ M or 1 mM). EtOH served as control (vehicle). Scale bar, 50 μ m. **(E)** Quantification of remaining soluble A β 40 in the supernatant of platelet culture using Western blot (n = 3).

2.5. A β Induced GPVI-Mediated ROS Production and Integrin $\alpha_{IIb}\beta_3$ Activation In Vitro

Platelets are metabolically active and display high adenosine triphosphate (ATP) turnover [25]. Luminometric analyses showed a significant reduction of the intracellular ATP level if dysfunction of complex III was induced by antimycin A (Figure 5A). Previously we demonstrated that A β 40 is able to induce the release of ATP and platelet aggregation [21,23]. Furthermore, ADP/ATP plays an important role in platelet-mediated A β aggregation [21] that was enhanced when mitochondrial dysfunction was reinforced by antimycin A (Figure 4A). Therefore, we investigated the effect of complex III dysfunction for A β 40-induced platelet aggregation and ATP release in the presence of antimycin A. Both, A β 40 and CRP induced release of ATP from platelets. In the presence of antimycin A, release of ATP was comparable to solvent control EtOH upon CRP (used as positive control) and A β 40 stimulation (Figure 5B). However, we measured the reduction of the intracellular ATP level (Figure 5A) and of the ATP release (Figure 5B) in response to A β 40 in the presence of solvent control EtOH. Next, we investigated whether or not the aggregation of platelets is altered by blocking of complex III in platelets. As shown in Figure 5C, platelet aggregation was not altered, either following CRP stimulation or A β 40 treatment (Figure 5C) when platelets were pre-incubated with antimycin A. Vitamin C was shown to reduce platelet-mediated A β aggregation in the presence and absence of antimycin A (Figure 4D), suggesting that ROS generation plays a crucial role in these processes. Moreover, integrin $\alpha_{IIb}\beta_3$ and GPVI play an important role in platelet-mediated A β aggregation [21,23]. Therefore, we incubated platelets with 5 and 10 μ M A β 40 and determined ROS generation in GPVI-deficient platelets from *Gp6^{-/-}* mice. As shown in Figure 5D, ROS generation of GPVI-deficient platelets was significantly reduced in response to A β 40 and CRP (positive control) (Figure 5D), suggesting that GPVI is involved in ROS-mediated A β aggregation facilitated by platelets. ROS production regulates integrin $\alpha_{IIb}\beta_3$ activation [32], a major contributor of platelet-mediated A β aggregation [21]. Therefore, we next determined integrin activation following A β stimulation in the presence and absence of the ROS scavenger vitamin C to investigate, if A β -induced ROS production is able to prompt integrin $\alpha_{IIb}\beta_3$ activation (Figure 5E). As shown in Figure 5E, pre-treatment with vitamin C led to reduced A β 40-induced activation of integrin $\alpha_{IIb}\beta_3$ in ADP-treated platelets (Figure 5E).

2.6. Mitochondrial ROS Production and Mitochondrial Membrane Potential in Platelets from Alzheimer's Disease Transgenic Mice APP23

In our previous studies we showed that aged mice (two years old) from the AD transgenic mouse line APP23, which develop amyloid- β deposits in the brain parenchyma and cerebral vessels at this age, exhibit pre-activated platelets in the blood circulation accompanied by enhanced integrin $\alpha_{IIb}\beta_3$ activation and degranulation of platelets compared to age-matched control mice [19]. Currently we analyzed mitochondria from APP23 mice using platelets from one- and two-year-old mice. Measurements using the ROS sensitive dye MitoSOX-Red showed that superoxide production in resting platelets from APP23 mice is comparable to resting platelets from WT mice (Figure 6A). The generation of mitochondrial superoxide in platelets was significantly increased when platelets were stimulated with 5 μ M A β 40 and even stronger with 20 μ M A β 40, as compared to resting platelets from one- and two-year-old APP23 and WT control mice. However, stimulation with 20 μ M A β 40 led to increased levels of superoxide in platelets from APP23 mice independent of their age, as compared to age-matched control mice (Figure 6A). The mitochondrial transmembrane potential ($\Delta\psi_m$) of non-stimulated (resting) platelets was comparable in platelets from one- and two-year-old APP23 and WT mice (Figure 6B). However, stimulation with 5 μ M A β 40 led to reduced mitochondrial transmembrane potential in platelets from WT mice (Figure 6B). Moreover, stimulation with 20 μ M A β 40 reduced mitochondrial transmembrane potential in platelets from one- and two-year-old WT mice (Figure 6B).

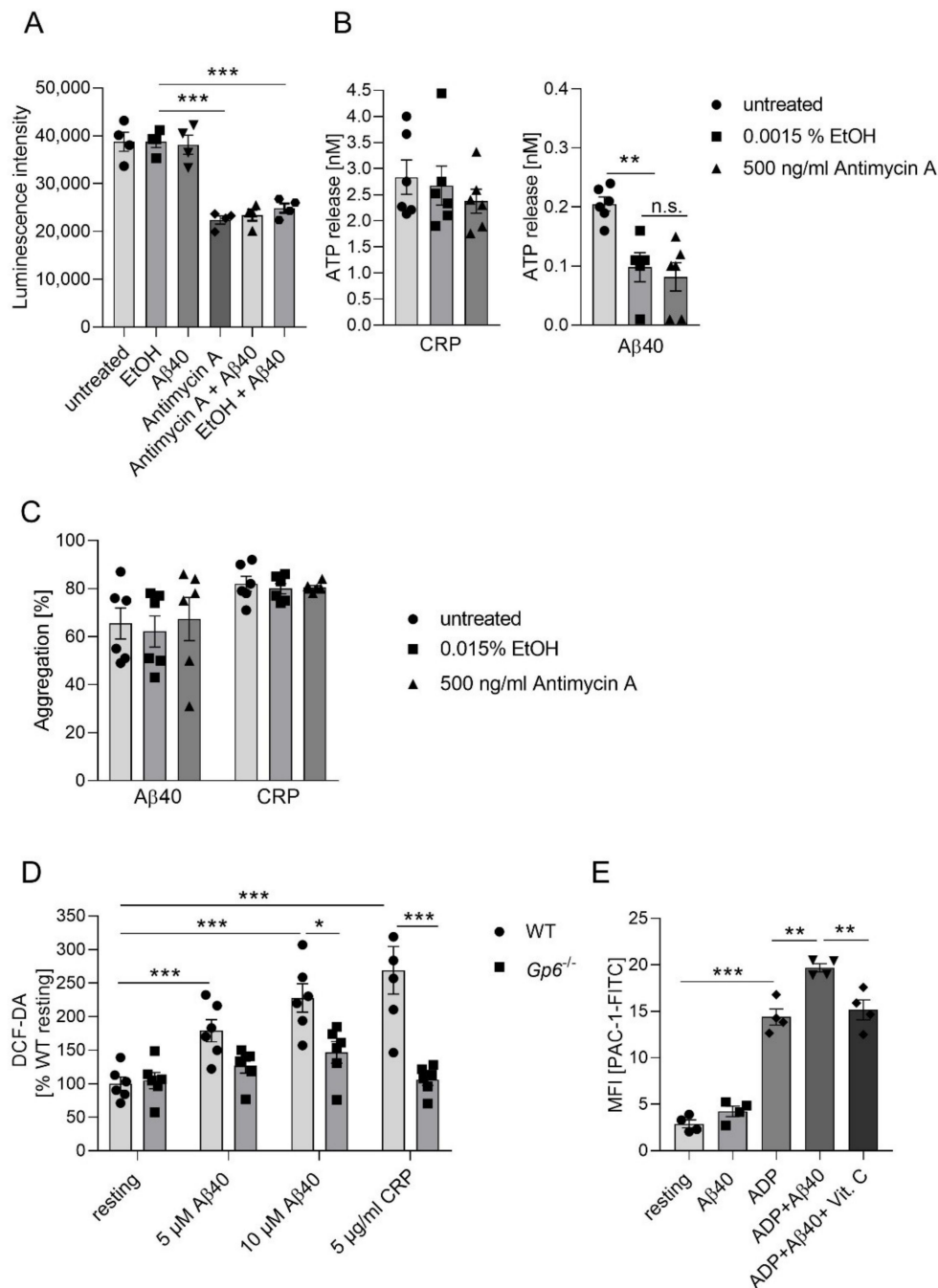


Figure 5. Impact of complex III inhibition on platelet functions following Aβ40 stimulation. **(A)** Detection of intracellular ATP levels after incubation of platelets with Aβ40 (5 μM), antimycin A (12.5 μM) and EtOH (as control, vehicle) for 90 min using Luminescence intensity (n = 4, *** = $p < 0.001$; two-way ANOVA with Tukey's multiple comparisons test). **(B)** Measurement of ATP release from antimycin A-pretreated platelets (EtOH was used in controls as vehicle) following Aβ40 (20 μM) or CRP (1 μg/mL) (n = 5–6). Analyses were performed using one-way ANOVA and Dunnett's multiple comparisons post-hoc test. ** $p < 0.01$; n.s.: not significant. **(C)** Aggregation of antimycin A-pretreated platelets upon Aβ40 (10 μM) or CRP (1 μg/mL). EtOH was used as control (vehicle) (n = 5–6). **(D)** Measurement of reactive oxygen species (ROS) generation with DCF-DA in GPVI-deficient platelets upon Aβ40 and CRP (n = 6). Data represent mean value ± SEM; two-way ANOVA with Sidak's multiple comparisons test. *** $p < 0.001$; ** $p < 0.01$; * $p < 0.05$. **(E)** Flow cytometric analysis of integrin activation at the surface of platelets using PAC-1 antibody upon stimulation with Aβ40 (11.5 μM) and ADP (5 μM). Where indicated, samples were pre-incubated with vitamin C (1 mM) for 30 min at RT (n = 4). Data represent mean value ± SEM; two-way ANOVA with Tukey's multiple comparisons test. *** $p < 0.001$; ** $p < 0.002$.

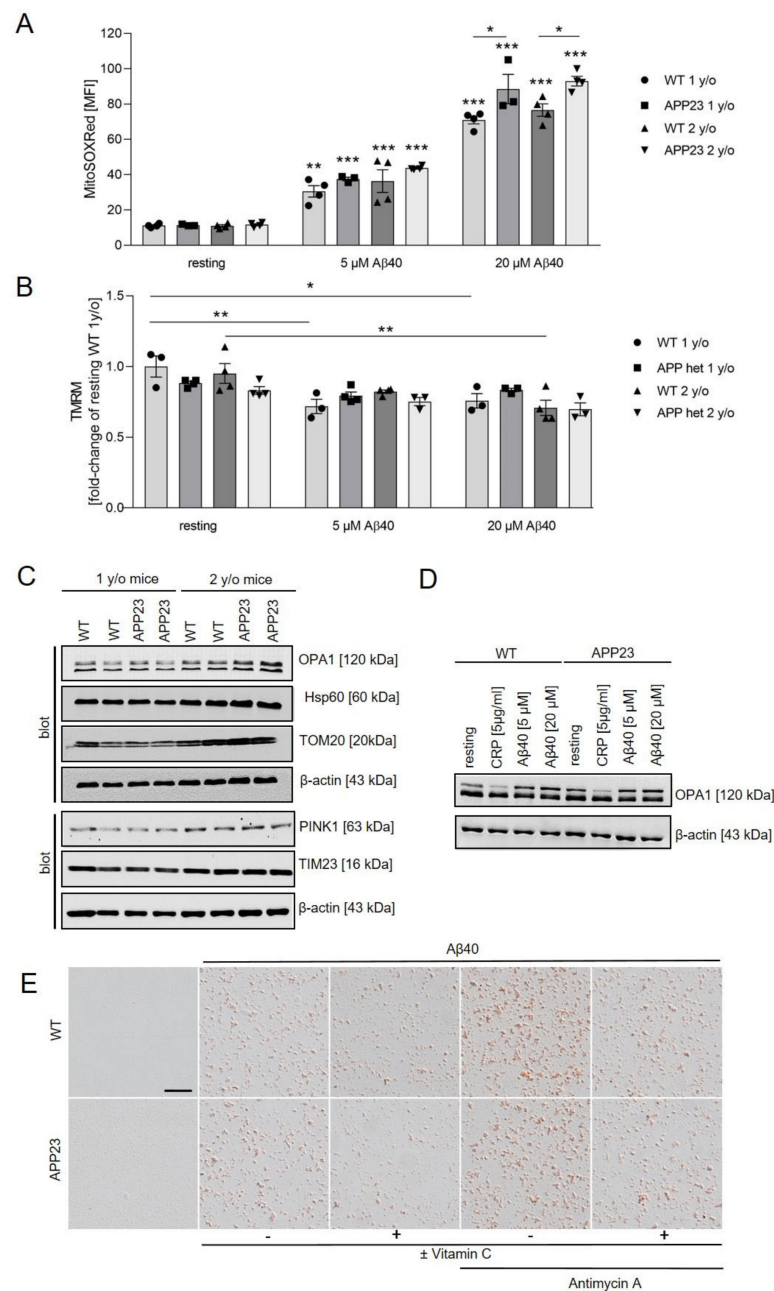


Figure 6. Analysis of mitochondrial function in platelets from APP23 mice. **(A,B)** Platelets from one- and two-year-old WT and APP23 mice were incubated with 5 and 20 μM Aβ40 for 30 min. Formation of superoxide was examined using MitoSOX™ Red and depolarization of platelet mitochondrial membrane was observed by decrease in TMRM fluorescence intensity. Data show the mean value ± SEM (n = 3–4), two-way ANOVA with Tukey’s multiple comparisons test. *** $p < 0.001$; ** $p < 0.01$; * $p < 0.05$; vs. basal or as indicated. **(C)** Expression levels of mitochondrial proteins in platelets from one- and two-year-old WT and APP23 mice were determined by Western blot analysis. β-actin served as loading control (n = 4). **(D)** Western blot analysis of the mitochondrial protein OPA1 in platelets from two-year-old WT and APP23 mice after stimulation with Aβ40 and CRP. β-actin served as loading control (n = 3). **(E)** Representative images of congo-red stained amyloid aggregates in the culture of platelets after incubation with soluble, synthetic Aβ40 (5 μM) for three days in the presence or absence of antimycin A (500 ng/mL) and vitamin C (100 μM). Platelets from one-year-old WT and APP23 mice were used (n = 3). Scale bar, 50 μm.

Furthermore, we analyzed the levels of mitochondrial proteins in platelets from one- and two-year-old APP23 mice in comparison to age-matched controls. Western blot analysis

revealed that expression of TOM20 and TIM23 was increased in APP23 and WT mice at the age of two years without reaching statistical significance. However, no alterations in protein expression was detected between platelets from different groups at the same age (Figure 6C and Figure S3). The eight splice variants and two proteolytic cleavage sites within mitochondrial OPA1 result in long and short forms of OPA1 with divergent functions in cristae biogenesis and mitochondrial fusion [33]. To investigate whether or not A β 40 induces the cleavage of OPA1 in platelets from WT and APP23 mice, we stimulated platelets with different concentrations of A β 40 and CRP as positive control. As shown in Figure 6D, protein levels of the long form of OPA1 was slightly increased following stimulation of platelets with A β 40 as compared to resting platelets but does not reach statistical significance (Figure S4). In contrast, the levels of the long form of OPA1 was slightly reduced in CRP-stimulated platelets but did not reach statistical significance (Figure 6D and Figure S4). We next analyzed platelet-mediated A β 40 aggregation in cell culture using platelets from age-matched APP23 and control mice. As already observed in cultured human platelets (Figure 4), treatment of murine platelets with antimycin A increased the formation of congo-red positive A β 40 aggregates, whereas treatment with vitamin C reduced the number of A β 40 aggregates. However, no differences were observed between platelets from APP23 and WT mice (Figure 6E).

3. Discussion

This study showed that stimulation of human platelets from healthy donors by A β 40 led to ROS and superoxide production, reduced mitochondrial transmembrane potential, induced the release of mitochondria from platelets and reduced the content of the mitochondrial protein TOM20. Furthermore, the oxygen consumption rate was reduced when we incubated platelets from healthy donors with A β 40 or A β 40 and CRP as deciphered by OCR. Enhanced mitochondrial dysfunction induced by antimycin A led to enhanced platelet-mediated A β 40 aggregate formation. This was due—at least in part—by GPVI- and ADP-mediated ROS production, leading to enhanced integrin $\alpha_{IIb}\beta_3$ activation in the presence of A β 40. A β 40 aggregate formation in presence of platelets were comparable between APP23 mice and WT controls, which could be reduced upon treatment with vitamin C.

In line with studies in the past [15], we currently observed that A β 40 induced ROS and depolarization of the mitochondrial membrane in platelets from healthy donors. In line with previous platelet activation and adhesion studies [22], A β 1-16 neither induced the formation of ROS and superoxide nor reduced mitochondrial transmembrane potential loss in platelets. This is due to the fact that the RHDS binding sequence of A β alone is not sufficient to induce A β -mediated alterations in platelets, including A β -induced outside-in signaling of integrin $\alpha_{IIb}\beta_3$. Thus, A β binding to integrin $\alpha_{IIb}\beta_3$ and integrin outside-in signaling might be important for superoxide production and dysregulation of mitochondrial membrane potential.

Platelet activation, including granular release and aggregation, are energy-dependent processes. Platelets are able to switch between glycolysis and oxidative phosphorylation using either glucose or fatty acids. Activation of platelets promotes a rapid uptake of exogenous glucose and display a glycolytic phenotype coupled with a minor rise in mitochondrial oxygen consumption [34]. To support platelet activation under nutrient limiting conditions, platelets are able to use glucose, glycogen or fatty acids. Thus, platelets have significant metabolic fuel and pathway flexibility, but mostly use glycolysis for ATP generation upon activation [34,35]. Therefore, we analyzed A β 40-induced release of ATP and platelet aggregation after inducing mitochondrial dysfunction using antimycin A that inhibits complex III of the mitochondrial respiratory chain. Treatment of platelets with antimycin A results in the reduction of the mitochondrial ATP production and supports ROS generation and mitochondrial dysfunction [36]. Treatment of platelets with high dose of antimycin A results in reduced collagen-induced platelet aggregation and strongly reduced dense granule secretion [37]. Here, we used low doses of antimycin A that is

able to amplify platelet-mediated A β 40 aggregate formation but did not alter platelet aggregation or ATP release, suggesting that ATP content in platelets is still sufficient to allow dense granule release and platelet aggregation.

Platelet-mediated A β 40 aggregate formation was amplified by mitochondrial dysfunction in a dose-dependent manner using antimycin A (Figures 4 and 6). The reduction of A β aggregation by vitamin C strongly indicates that A β -induced ROS production in platelets is responsible for platelet-mediated A β aggregate formation. Vitamin C is an antioxidant and its protective effects and clinical relevance for AD has been already shown in different studies in the past [38–40]. Treatment of human and murine platelets with vitamin C reduced the formation of A β aggregates (Figures 4 and 6). In particular, enhanced A β aggregate formation following mitochondrial dysfunction by antimycin A treatment was strongly reduced in the presence of vitamin C, demonstrating that the reduction of free radical generation attenuates platelet-mediated A β aggregate formation. Thus, enhanced ROS level in AD patients might be critical for platelet-mediated A β aggregate formation in cerebral vessels known as cerebral amyloid angiopathy (CAA) [41]. Our data suggests that vitamin C might reduce platelet-mediated effects on CAA even in the presence of already existing A β aggregates, because positive effects of vitamin C on the reduction of A β aggregates were also observed with platelets from APP23 mice (Figure 6).

Mitochondrial dysfunction resulting in increased ROS generation accounts for platelet-mediated A β aggregate formation in vitro. Similarly, in HEK293 cells, mitochondrial ROS production enhanced the formation of A β [31]. In contrast to the present study, the authors provide evidence that ROS induced elevated processing of amyloid precursor protein (APP) and that, in turn, A β led to mitochondrial dysfunction and increased ROS levels, suggesting a vicious cycle that contributes to the pathology of AD. Here, we observed that ROS is responsible for A β aggregate formation but not for the formation of endogenous A β by APP processing in platelets. The source of A β 40 in plasma is highly discussed among researchers. Chen and colleagues believe that platelets are the primary source of amyloid beta-peptide in human blood [14]. Wisniewski and Wegiel think that vascular A β originates from a different source to A β in plaques and is generated locally, principally in smooth muscle cells [42]. The group of M. Jucker believes that, although several factors may contribute to CAA in humans, the neuronal origin of transgenic APP, high levels of A β in cerebrospinal fluid and regional localization of CAA in APP23 transgenic mice indicate that neuron-derived A β can migrate to and accumulate in the vasculature far from its production site. Thus, A β transport and drainage pathways, rather than local production of A β by platelets or smooth muscle cells, are a primary mechanism underlying CAA formation [43,44]. Results of our previous studies demonstrate that platelet-mediated A β 40 fibril formation and aggregation is not altered when we inhibited the A β production from APP precursors using inhibitors. This indicates that A β 40 of platelet origin does not contribute to A β 40 aggregation in the platelet culture [15].

We have recently shown that GPVI, ADP and integrin $\alpha_{IIb}\beta_3$ are involved in platelet-mediated A β aggregate formation by direct binding of A β to GPVI and integrin $\alpha_{IIb}\beta_3$ followed by the release of ATP/ADP [21,23]. Here, our data indicates that GPVI is also responsible for A β -induced ROS production and that ROS production is involved in $\alpha_{IIb}\beta_3$ integrin activation induced by ADP and A β (Figure 5). Integrin activation of platelets by ROS has already been shown earlier [32]. However, the authors used thrombin to produce ROS in platelets but not soluble A β as shown here. GPVI-triggered ROS production and enhanced integrin activation might support A β binding to integrin $\alpha_{IIb}\beta_3$ and to GPVI to reinforce platelet-mediated A β aggregate formation. Furthermore, the release of mitochondria following treatment of platelets with soluble A β might contribute to enhanced platelet activation and inflammation in AD [30].

Mitochondrial dysfunction has been shown to contribute to the pathogenesis of AD and is responsible for the decrease in respiration as observed in platelets from AD patients [26]. However, Fisar and colleagues found no correlation between dysfunctional mitochondrial respiration and changes in plasma A β levels as found in patients with

AD [27]. Our data indicates that incubation of platelets from healthy volunteers with A β or A β and CRP significantly reduced mitochondrial respiration compared to CRP alone, suggesting that A β itself is responsible for defects in mitochondrial respiration and that enhanced A β plasma levels might affect mitochondrial respiration of circulating platelets in AD transgenic mice and patients.

In AD patients and transgenic mice (APP23), enhanced platelet activation was detected [18,19]. Treatment of APP23 mice with the anti-platelet drug clopidogrel reduced the formation of CAA suggesting that enhanced platelet activation contributes to the pathology of AD [21]. The impact of enhanced platelet activation and mitochondrial dysfunction has already been described in different diseases [45–48]. Patients with sickle cell disease are characterized by decreased mitochondrial respiration, mitochondrial dysfunction that correlates with enhanced platelet activation and hemolysis both contributing to the pathogenesis of the disease [46]. Dengue infection is accompanied by enhanced activation and mitochondrial dysfunction of platelets [47]. In septic patients, Puskarich and colleagues found a correlation between platelet mitochondrial function and organ failure with increased respiratory rates in non-survivors compared to survivors [48]. In diabetes, hyperglycemia was associated with enhanced collagen-induced platelet activation that was triggered by mitochondrial superoxide production [45]. Furthermore, enhanced levels of ROS induced oxidative stress, which plays a crucial role in tissue damage after brain ischemia/reperfusion [49,50].

Taken together, platelet-mediated A β 40 aggregate formation is enhanced by mitochondrial dysfunction through GPVI-mediated ROS production and elevated integrin $\alpha_{IIb}\beta_3$ activation. Thus, mitochondrial dysfunction contributes to platelet-mediated A β aggregate formation, and might be not only a beneficial biomarker but also a promising target to limit platelet activation exaggerated pathological manifestations in AD.

4. Materials and Methods

4.1. Chemicals, Peptides and Antibodies

Platelets were activated with collagen-related peptide (= CRP, Richard Farndale, University of Cambridge, United Kingdom), synthetic A β 40 (1-40; Bachem, Switzerland, cat no 4014442.1000) sequence single-letter code (DAEFRHDSGYEVHHQKLVFFAEDVGSNKGAIIGLMVGGVV), A β 16 (A β 1-16, Bachem, Switzerland) ADP (Sigma-Aldrich). Apyrase (grade II, from potato) and prostacyclin from Calbiochem were used for isolation. Antimycin A (*Streptomyces* sp., A8674-25MG, Sigma-Aldrich, St. Louis, USA) was solved in 95% EtOH. Vitamin C (L(+)-Ascorbic acid) is from VWR Chemicals. Antibodies: Hsp60 (SAB 4501464; Sigma Aldrich, dilution 1:1000), OPA1 (sc-393296, Santa Cruz, dilution 1:500), PINK1 (D8G Rabbit mAb 6946; Cell Signalling, dilution 1:500), TIM23 (BD 611222; BD Biosciences, dilution 1:500), TOM20 (sc-11415; Santa Cruz, dilution 1:500), Amyloid- β (6E10, SIG-39320; Covance, dilution 1:2000). The antibodies β -actin (cat no 4967) and horseradish peroxidase (HRP)-linked secondary antibodies (cat no 7074 and cat no 7076) were from Cell Signaling Technology.

4.2. Animals

Heterozygous C57BL/6J-TgN(Thy1.2-hAPP751-KM670/671 NL)23 (APP23) were provided by Novartis Pharma AG. Mice with targeted deletion of GPVI were provided by J. Ware (University of Arkansas for Medical Sciences) and backcrossed to C57BL/6 mice. All animal experiments were conducted according the Declaration of Helsinki and approved by the Ethics Committee of the State Ministry of Agriculture, Nutrition and Forestry State of North Rhine-Westphalia, Germany (reference number: AZ 84-02.05.40.16.073). Mice were maintained in a specific pathogen-free environment and fed standard mouse diet ad libitum.

4.3. Murine Platelet Preparation

Platelets were prepared as previously described [23]. Murine blood was taken from the retro-orbital-plexus in a tube containing heparin and centrifuged at $250\times g$ for 5 min at room temperature. Platelet-rich-plasma was obtained by centrifugation at $50\times g$ for 6 min and was washed twice with Tyrode's buffer (136 mM NaCl, 0.4 mM Na_2HPO_4 , 2.7 mM KCl, 12 mM NaHCO_3 , 0.1% glucose, 0.35% bovine serum albumin (BSA, Sigma-Aldrich, St. Louis, MO, USA), pH 7.4) in the presence of prostacyclin (0.5 μM) and apyrase (0.02 U/mL) at $650\times g$ for 5 min at room temperature. Before use, platelet pellets were resuspended in the Tyrode's buffer (without prostacyclin and apyrase) supplemented with 1 mM CaCl_2 .

4.4. Human Platelet Preparation

Platelets were prepared as previously described [23]. ACD-anticoagulated blood was obtained from healthy volunteers between the ages of 18 and 50 years old from the blood bank. Donors provided written informed consent to participate in this study according to the Ethics Committee and the Declaration of Helsinki (study number 2018-140-KFogU). The blood was centrifuged at $200\times g$ for 10 min at room temperature. The platelet-rich plasma (PRP) was added to phosphate buffered saline (PBS; pH 6.5, apyrase: 2.5 U/mL and 1 μM PGI_2) in 1:1 volumetric ratio and centrifuged at $1000\times g$ for 6 min. Platelets were resuspended in Tyrode's-buffer (140 mM NaCl; 2.8 mM KCl; 12 mM NaHCO_3 ; 0.5 mM Na_2HPO_4 ; 5.5 mM glucose pH 7.4).

4.5. Human and Murine Platelet Culture

Isolated human or murine platelets at the concentration of 2×10^6 platelets/well were added to 150 μL of DMEM medium (Dulbecco's modified Eagle's medium, 41965-039; Life Technologies). Platelets were incubated with 5 μM synthetic $\text{A}\beta_{40}$ in the presence of antimycin A (or EtOH as solvent control) and Vitamin C for 3 days at 37°C and 5% CO_2 . After 3 days, the supernatants of cell culture were collected for determination of remaining $\text{A}\beta$ concentration using immunoblot analysis. The supernatants were prepared with reducing sample buffer (Laemmli buffer) and denatured at 95°C for 5 min. Unbound platelets were removed by rinsing with PBS and adherent platelets were fixed with 2% paraformaldehyde and stained against fibrillary $\text{A}\beta$ aggregates with Congo red according to the manufacturer's protocol (Millipore cat no 101641).

4.6. Measurement of Intracellular ROS Level

Washed platelets were added to DMEM medium (Dulbecco's modified Eagle's medium) and incubated with different concentrations of $\text{A}\beta_{40}$ or $\text{A}\beta_{16}$ (as control) for 24 h at 37°C . After incubation, platelets were loaded with 10 μM DCF-DA (2',7'-Dichlor-dihydrofluorescein-diacetat; D6883; Sigma-Aldrich) at 37°C for 15 min in the dark. Reaction was stopped using PBS. Samples were analyzed on a FACSCalibur flow cytometer (BD Biosciences).

4.7. Measurement of Mitochondrial Superoxide

Washed platelets were pre-incubated with MitoSOXTM Red (M36008; Invitrogen) at room temperature for 30 min in the dark. Then, platelets were stimulated with $\text{A}\beta_{40}$ or $\text{A}\beta_{16}$ (as control) for 30 min at RT. Reaction was stopped using PBS. Samples were analyzed on a FACSCalibur flow cytometer (BD Biosciences).

4.8. Measurement of Mitochondrial Membrane Potential

Isolated platelets were treated with $\text{A}\beta_{40}$ for 30 min at RT and then incubated with 100 nM tetramethylrhodamin methyl ester (TMRM; Sigma-Aldrich) in the dark. The reaction was stopped after 30 min incubation using PBS. Samples were analyzed on a FACSCalibur flow cytometer (BD Biosciences).

4.9. Measurement of Mitochondria Release Using MitoTracker™ Green FM

Human isolated platelets were incubated with 100 nM MitoTracker™ green FM (M7514; Invitrogen) for 30 min at 37 °C under exclusion of light. After incubation, platelets were stimulated with thrombin (0.1 U/mL or 0.5 U/mL) or A β 40 (2.3 μ M or 11.5 μ M for 15 min, 1 h and 4 h at RT in the dark. The reaction was stopped with PBS. Samples were analyzed on a FACSCalibur flow cytometer (BD Biosciences).

4.10. Cell Lysis and Immunoblotting

Human isolated platelets were stimulated with collagen-related peptide (CRP, 1 μ g/mL) or A β 40 (5 μ M or 20 μ M) at 37 °C with stirring (250 r.p.m) for 1 and 2 h. Stimulation was terminated with 5 \times ice-cold lysis buffer (100 mM Tris-HCl, 725 mM NaCl, 20 mM EDTA, 5% TritonX-100, complete protease inhibitor (PI) cocktail). Murine platelets were lysed with lysis buffer (15 mM Tris-HCl, 155 mM NaCl, 1 mM EDTA, 0.005% NaN₃, 5% IGPAL and PI). Cell lysates were prepared by boiling a sample of lysate with sodium dodecyl sulfate (SDS) sample buffer. Platelet lysates were then separated by SDS-polyacrylamide gel electrophoresis, electro-transferred onto nitrocellulose blotting membrane (GE Healthcare Life Sciences). Membrane was blocked using 5% nonfat dry milk in TBST (tris-buffered saline with 0.1% Tween20) and probed with the appropriate primary antibody and secondary antibody HRP-conjugated antibody. Immunoreactive bands were visualized with enhanced chemiluminescence detection reagents using FusionFX Chemiluminescence Imager Systems (Vilber) and quantified using the FUSION FX7 software (Vilber).

4.11. Platelet Aggregation

Platelet aggregation was measured as percentage light transmission compared to Tyrode's buffer (=100%) using Chrono-Log dual channel lumi-aggregometer (model 700) at 37 °C stirring at 1000 rpm. Where indicated, the platelets (20 \times 10³ cells/ μ L) were pre-treated with 500 ng/mL antimycin A or 0.0015% EtOH (as solvent control) for 1 h at RT. Platelets were then stimulated with 1 μ g/mL CRP or 10 μ M A β 40 and aggregation response was examined.

4.12. Measurement of Intracellular ATP Level and ATP Release

Intracellular ATP level was measured using Mitochondrial ToxGlo™ Assay (Promega) following the manufacturer's protocol. Platelets were adjusted to a final concentration of 2 \times 10² and incubated with 5 μ M A β 40 and 12.5 antimycin A (EtOH used as control) for 90 min at 37 °C. ATP release was measured using ChronoLume luciferin assay (ChronoLog) on a LumiAggregometer (model 700, ChronoLog) at 37 °C stirring at 1000 rpm. Where indicated, the platelets (20 \times 10³ cells/ μ L) were pre-treated with 500 ng/mL antimycin A or 0.0015% EtOH (as solvent control) for 1 h at RT. After 2 min of incubation with luciferase, platelets were stimulated with 1 μ g/mL CRP or 20 μ M A β 40 and monitored for ATP release.

4.13. A β 40 Quantification by Enzyme-Linked Immunosorbent Assay (ELISA)

Platelets were adjusted to a final concentration of 1 \times 10⁶ / μ L and pre-incubated with 500 ng/mL antimycin A or 0.0015% EtOH (as solvent control) for 24 h at 37 °C. Incubation was terminated with 5 \times ice-cold lysis buffer (100 mM Tris-HCl, 725 mM NaCl, 20 mM EDTA, 5% TritonX-100, complete protease inhibitor (PI) cocktail). After centrifugation, A β 40 levels in supernatants were measured following the manufacturer's protocol (human A β 1-40 ELISA Kit, Cat. No: MBS2506221, MyBioSource).

4.14. Measurement of the Oxygen Consumption Rate

Mitochondrial respiration of blood platelets was analyzed by using the Seahorse XFe96 extracellular flux analyzer and the Seahorse XF Cell Mito Stress Test Kit (103015-100, Agilent Technologies), purchased from Agilent (Agilent Technologies, Santa Clara, CA, USA). The Seahorse XF Cell Mito Stress Test Kit allows direct measurement of mitochondrial function

in living cells by monitoring the oxygen consumption rate (OCR) and was performed according to the manufacturers' guidelines. ACD-anticoagulated human whole blood samples were obtained from healthy volunteers. Blood was centrifuged at 200 g for 20 min at 22 °C without brake. The platelet-rich-plasma, PRP thus obtained was separated and added to phosphate buffered saline (PBS, pH 6.5), supplemented with apyrase (2.5 U/mL) and prostaglandin I₂ (PGI₂, 1 µM) in a volumetric ratio of 1:10 and centrifuged at 1000 g for 10 min at 22 °C without brake. Washed platelets were subsequently resuspended in Seahorse XF DMEM medium (containing 5.5 mM D-Glucose, 1 mM Na-Pyruvate, 4 mM L-Glutamine, pH 7.4). Afterwards, platelets were seeded in a density of 2×10^7 cells/well into a Cell-Tak (100 µg/mL) coated XFe96 cell culture microplate in Seahorse XF DMEM medium (containing 5.5 mM D-Glucose, 1 mM Na-Pyruvate, 4 mM L-Glutamine, pH 7.4). To evaluate the impact of Aβ40 on mitochondrial respiration using OCR as a readout, the Seahorse XF DMEM medium was either supplemented with 5 µM Aβ40 or without (Bachem, Switzerland). For optimal adhesion, the seeded platelets were centrifuged in two steps at 143 and 213 × g respectively for one min each. After centrifugation, the cells were incubated for 30 min in a non-CO₂ incubator at 37 °C, prior the start of the assay. Initially the basal OCR was measured, followed by sequential injections of CRP (5 µg/mL), oligomycin (1 µM), FCCP (0.5 µM) and a mix of antimycin A and rotenone (each 1 µM). ATP-linked respiration is defined as the difference of the last rate measurement before oligomycin injection and the minimum rate measurement after oligomycin injection. Proton leak is defined as the minimum rate measurement after oligomycin minus non-mitochondrial respiration. The OCR measurements were conducted in 3 cycles for each condition. All data were analyzed using the wave software (Agilent Technologies, 2.6.1).

4.15. Flow Cytometry Measurement of PAC-1 Binding

Flow cytometry analysis of platelet activation was performed using fluorophore-labeled antibody PAC-1 (activated integrin $\alpha_{IIb}\beta_3$ receptor marker, BD Biosciences). A total of 5 µL of whole blood was added to tube containing phosphate-buffered saline (PBS), antibody and agonists (ADP and Aβ40). Where indicated, whole blood was pre-incubated with vitamin C (1 mM) for 30 min at RT. After incubation at room temperature for 15 min, the reaction was stopped by the addition of PBS and samples were analyzed on a FACSCalibur flow cytometer (BD Biosciences).

Supplementary Materials: The following are available online at <https://www.mdpi.com/article/10.3390/ijms22179633/s1>.

Author Contributions: L.D., T.F., L.M.T. and C.F. performed experiments and analyzed the data. L.D. and M.E. designed experiments, discussed the data and wrote the manuscript. A.S.R. discussed experimental designs and data, read and edited the manuscript. M.C. discussed the data, read and edited the manuscript. All authors have read and agreed to the published version of the manuscript.

Funding: This research was funded by grant from the German Research Foundation (Deutsche Forschungsgemeinschaft, DFG, grant number EL651/5-1) and by the *Stiftung für Altersforschung* of the Heinrich-Heine University Düsseldorf) to M.E., and by the *Forschungskommission* of the Medical Faculty Düsseldorf (grant 2020/09) to L.D.

Institutional Review Board Statement: Fresh ACD-anticoagulated blood was obtained from healthy volunteers between the ages of 18 und 50 years old. Participants provided their written informed consent to participate in this study according to the Ethics Committee and the Declaration of Helsinki (study number 2018-140-KFogU). All animal experiments were conducted according the Declaration of Helsinki and approved by the Ethics Committee of the State Ministry of Agriculture, Nutrition and Forestry State of North Rhine-Westphalia, Germany (reference number: AZ 84-02.05.40.16.073).

Informed Consent Statement: Informed consent was obtained from all subjects involved in the study.

Data Availability Statement: The data presented in this study are available on request from the corresponding author.

Acknowledgments: We thank Martina Spelleken for providing outstanding technical assistance and Nahal Brocke-Ahmadinejad and the ‘Cellular Metabolism Platform’ of the Institute of Bio-chemistry and Molecular Biology I, Medical Faculty, Heinrich-Heine-University Düsseldorf, Germany for introduction into the Seahorse Flux Analyzer.

Conflicts of Interest: The authors declare no conflict of interest.

References

1. Selkoe, D.J.; Hardy, J. The amyloid hypothesis of Alzheimer’s disease at 25 years. *EMBO Mol. Med.* **2016**, *8*, 595–608. [[CrossRef](#)] [[PubMed](#)]
2. Reddy, P.H.; Oliver, D.M. Amyloid Beta and Phosphorylated Tau-Induced Defective Autophagy and Mitophagy in Alzheimer’s Disease. *Cells* **2019**, *8*, 488. [[CrossRef](#)] [[PubMed](#)]
3. Reddy, P.H.; Tripathi, R.; Troung, Q.; Tirumala, K.; Reddy, T.P.; Anekonda, V.; Shirendeb, U.P.; Calkins, M.J.; Reddy, A.P.; Mao, P.; et al. Abnormal mitochondrial dynamics and synaptic degeneration as early events in Alzheimer’s disease: Implications to mitochondria-targeted antioxidant therapeutics. *Biochim. Biophys. Acta* **2012**, *1822*, 639–649. [[CrossRef](#)] [[PubMed](#)]
4. Du, H.; Guo, L.; Yan, S.; Sosunov, A.A.; McKhann, G.M.; Yan, S.S. Early deficits in synaptic mitochondria in an Alzheimer’s disease mouse model. *Proc. Natl. Acad. Sci. USA* **2010**, *107*, 18670–18675. [[CrossRef](#)]
5. Cai, Q.; Tammineni, P. Alterations in Mitochondrial Quality Control in Alzheimer’s Disease. *Front. Cell. Neurosci.* **2016**, *10*, 24. [[CrossRef](#)]
6. Shefa, U.; Jeong, N.Y.; Song, I.O.; Chung, H.J.; Kim, D.; Jung, J.; Huh, Y. Mitophagy links oxidative stress conditions and neurodegenerative diseases. *Neural Regen. Res.* **2019**, *14*, 749–756.
7. Manczak, M.; Calkins, M.J.; Reddy, P.H. Impaired mitochondrial dynamics and abnormal interaction of amyloid beta with mitochondrial protein Drp1 in neurons from patients with Alzheimer’s disease: Implications for neuronal damage. *Hum. Mol. Genet.* **2011**, *20*, 2495–2509. [[CrossRef](#)]
8. Reddy, P.H.; Manczak, M.; Yin, X.; Grady, M.C.; Mitchell, A.; Tonk, S.; Kuruva, C.S.; Bhatti, J.S.; Kandimalla, R.; Vijayan, M.; et al. Protective Effects of Indian Spice Curcumin Against Amyloid- β in Alzheimer’s Disease. *J. Alzheimer’s Dis.* **2018**, *61*, 843–866. [[CrossRef](#)]
9. Reddy, P.H.; Williams, J.; Smith, F.; Bhatti, J.S.; Kumar, S.; Vijayan, M.; Kandimalla, R.; Kuruva, C.S.; Wang, R.; Manczak, M.; et al. MicroRNAs, Aging, Cellular Senescence, and Alzheimer’s Disease. *Prog. Mol. Biol. Transl. Sci.* **2017**, *146*, 127–171.
10. Reddy, P.H.; McWeeney, S.; Park, B.S.; Manczak, M.; Gutala, R.V.; Partovi, D.; Jung, Y.; Yau, V.; Searles, R.; Mori, M.; et al. Gene expression profiles of transcripts in amyloid precursor protein transgenic mice: Up-regulation of mitochondrial metabolism and apoptotic genes is an early cellular change in Alzheimer’s disease. *Hum. Mol. Genet.* **2004**, *13*, 1225–1240. [[CrossRef](#)]
11. Kerr, J.S.; Adriaanse, B.A.; Greig, N.H.; Mattson, M.P.; Cader, M.Z.; Bohr, V.A.; Fang, E.F. Mitophagy and Alzheimer’s Disease: Cellular and Molecular Mechanisms. *Trends Neurosci.* **2017**, *40*, 151–166. [[CrossRef](#)]
12. Sheng, Z.H.; Cai, Q. Mitochondrial transport in neurons: Impact on synaptic homeostasis and neurodegeneration. *Nat. Rev. Neurosci.* **2012**, *13*, 77–93. [[CrossRef](#)] [[PubMed](#)]
13. Li, Q.X.; Whyte, S.; Tanner, J.E.; Evin, G.; Beyreuther, K.; Masters, C.L. Secretion of Alzheimer’s disease A β amyloid peptide by activated human platelets. *Lab. Investig. A J. Tech. Methods Pathol.* **1998**, *78*, 461–469.
14. Chen, M.; Inestrosa, N.C.; Ross, G.S.; Fernandez, H.L. Platelets are the primary source of amyloid beta-peptide in human blood. *Biochem. Biophys. Res. Commun.* **1995**, *213*, 96–103. [[CrossRef](#)]
15. Gowert, N.S.; Donner, L.; Chatterjee, M.; Eisele, Y.S.; Towhid, S.T.; Munzer, P.; Walker, B.; Ogorek, I.; Borst, O.; Grandoch, M.; et al. Blood platelets in the progression of Alzheimer’s disease. *PLoS ONE* **2014**, *9*, e90523. [[CrossRef](#)]
16. Zainaghi, I.A.; Talib, L.L.; Diniz, B.S.; Gattaz, W.F.; Forlenza, O.V. Reduced platelet amyloid precursor protein ratio (APP ratio) predicts conversion from mild cognitive impairment to Alzheimer’s disease. *J. Neural Transm.* **2012**, *119*, 815–819. [[CrossRef](#)]
17. Johnston, J.A.; Liu, W.W.; Coulson, D.T.; Todd, S.; Murphy, S.; Brennan, S.; Foy, C.J.; Craig, D.; Irvine, G.B.; Passmore, A.P. Platelet beta-secretase activity is increased in Alzheimer’s disease. *Neurobiol. Aging* **2008**, *29*, 661–668. [[CrossRef](#)]
18. Stellos, K.; Panagiota, V.; Kogel, A.; Leyhe, T.; Gawaz, M.; Laske, C. Predictive value of platelet activation for the rate of cognitive decline in Alzheimer’s disease patients. *J. Cereb. Blood Flow Metab.* **2010**, *30*, 1817–1820. [[CrossRef](#)]
19. Jarre, A.; Gowert, N.S.; Donner, L.; Munzer, P.; Klier, M.; Borst, O.; Schaller, M.; Lang, F.; Korth, C.; Elvers, M. Pre-activated blood platelets and a pro-thrombotic phenotype in APP23 mice modeling Alzheimer’s disease. *Cell Signal.* **2014**, *26*, 2040–2050. [[CrossRef](#)]
20. Prodan, C.I.; Ross, E.D.; Vincent, A.S.; Dale, G.L. Rate of progression in Alzheimer’s disease correlates with coated-platelet levels—A longitudinal study. *Transl. Res. J. Lab. Clin. Med.* **2008**, *152*, 99–102. [[CrossRef](#)] [[PubMed](#)]
21. Donner, L.; Falker, K.; Gremer, L.; Klinker, S.; Pagani, G.; Ljungberg, L.U.; Lothmann, K.; Rizzi, F.; Schaller, M.; Gohlke, H.; et al. Platelets contribute to amyloid-beta aggregation in cerebral vessels through integrin α IIb β 3-induced outside-in signaling and clusterin release. *Sci. Signal.* **2016**, *9*, ra52. [[CrossRef](#)]
22. Donner, L.; Gremer, L.; Ziehm, T.; Gertzen, C.G.W.; Gohlke, H.; Willbold, D.; Elvers, M. Relevance of N-terminal residues for amyloid-beta binding to platelet integrin α IIb β 3, integrin outside-in signaling and amyloid-beta fibril formation. *Cell Signal.* **2018**, *50*, 121–130. [[CrossRef](#)]

23. Donner, L.; Toska, L.M.; Krüger, I.; Gröniger, S.; Barroso, R.; Burleigh, A.; Mezzano, D.; Pfeiler, S.; Kelm, M.; Gerdes, N.; et al. The collagen receptor glycoprotein VI promotes platelet-mediated aggregation of β -amyloid. *Sci. Signal.* **2020**, *13*, eaba9872. [[CrossRef](#)]
24. Hayashi, T.; Tanaka, S.; Hori, Y.; Hirayama, F.; Sato, E.F.; Inoue, M. Role of mitochondria in the maintenance of platelet function during in vitro storage. *Transfus. Med.* **2011**, *21*, 166–174. [[CrossRef](#)]
25. Melchinger, H.; Jain, K.; Tyagi, T.; Hwa, J. Role of Platelet Mitochondria: Life in a Nucleus-Free Zone. *Front. Cardiovasc. Med.* **2019**, *6*, 153. [[CrossRef](#)]
26. Fišar, Z.; Hroudová, J.; Hansíková, H.; Spáčilová, J.; Lelková, P.; Wenchich, L.; Jiráček, R.; Zvěřová, M.; Zeman, J.; Martásek, P.; et al. Mitochondrial Respiration in the Platelets of Patients with Alzheimer's Disease. *Curr. Alzheimer Res.* **2016**, *13*, 930–941. [[CrossRef](#)]
27. Fišar, Z.; Jiráček, R.; Zvěřová, M.; Setnička, V.; Habartová, L.; Hroudová, J.; Vaníčková, Z.; Raboch, J. Plasma amyloid beta levels and platelet mitochondrial respiration in patients with Alzheimer's disease. *Clin. Biochem.* **2019**, *72*, 71–80. [[CrossRef](#)] [[PubMed](#)]
28. Cardoso, S.M.; Proença, M.T.; Santos, S.; Santana, I.; Oliveira, C.R. Cytochrome c oxidase is decreased in Alzheimer's disease platelets. *Neurobiol. Aging* **2004**, *25*, 105–110. [[CrossRef](#)]
29. Masselli, E.; Pozzi, G.; Vaccarezza, M.; Mirandola, P.; Galli, D.; Vitale, M.; Carubbi, C.; Gobbi, G. ROS in Platelet Biology: Functional Aspects and Methodological Insights. *Int. J. Mol. Sci.* **2020**, *21*, 4866. [[CrossRef](#)] [[PubMed](#)]
30. Boudreau, L.H.; Duchez, A.C.; Cloutier, N.; Soulet, D.; Martin, N.; Bollinger, J.; Pare, A.; Rousseau, M.; Naika, G.S.; Levesque, T.; et al. Platelets release mitochondria serving as substrate for bactericidal group IIA-secreted phospholipase A2 to promote inflammation. *Blood* **2014**, *124*, 2173–2183. [[CrossRef](#)] [[PubMed](#)]
31. Leuner, K.; Schutt, T.; Kurz, C.; Eckert, S.H.; Schiller, C.; Occhipinti, A.; Mai, S.; Jendrach, M.; Eckert, G.P.; Kruse, S.E.; et al. Mitochondrion-derived reactive oxygen species lead to enhanced amyloid beta formation. *Antioxid. Redox Signal.* **2012**, *16*, 1421–1433. [[CrossRef](#)] [[PubMed](#)]
32. Begonja, A.J.; Gambaryan, S.; Geiger, J.; Aktas, B.; Pozgajova, M.; Nieswandt, B.; Walter, U. Platelet NAD(P)H-oxidase-generated ROS production regulates α IIb β 3-integrin activation independent of the NO/cGMP pathway. *Blood* **2005**, *106*, 2757–2760. [[CrossRef](#)] [[PubMed](#)]
33. Del Dotto, V.; Fogazza, M.; Carelli, V.; Rugolo, M.; Zanna, C. Eight human OPA1 isoforms, long and short: What are they for? *Biochim. Biophys. Acta Bioenerg.* **2018**, *1859*, 263–269. [[CrossRef](#)] [[PubMed](#)]
34. Aibibula, M.; Naseem, K.M.; Sturmey, R.G. Glucose metabolism and metabolic flexibility in blood platelets. *J. Thromb. Haemost.* **2018**, *16*, 2300–2314. [[CrossRef](#)] [[PubMed](#)]
35. Zharikov, S.; Shiva, S. Platelet mitochondrial function: From regulation of thrombosis to biomarker of disease. *Biochem. Soc. Trans.* **2013**, *41*, 118–123. [[CrossRef](#)] [[PubMed](#)]
36. Wang, L.; Duan, Q.; Wang, T.; Ahmed, M.; Zhang, N.; Li, Y.; Li, L.; Yao, X. Mitochondrial Respiratory Chain Inhibitors Involved in ROS Production Induced by Acute High Concentrations of Iodide and the Effects of SOD as a Protective Factor. *Oxidative Med. Cell. Longev.* **2015**, *2015*, 217670. [[CrossRef](#)]
37. Rusak, T.; Tomasiak, M.; Ciborowski, M. Peroxynitrite can affect platelet responses by inhibiting energy production. *Acta Biochim. Pol.* **2006**, *53*, 769–776. [[CrossRef](#)]
38. Heo, J.H.; Hyon, L.; Lee, K.M. The possible role of antioxidant vitamin C in Alzheimer's disease treatment and prevention. *Am. J. Alzheimer's Dis. Other Dement.* **2013**, *28*, 120–125. [[CrossRef](#)]
39. Huang, J.; May, J.M. Ascorbic acid protects SH-SY5Y neuroblastoma cells from apoptosis and death induced by beta-amyloid. *Brain Res.* **2006**, *1097*, 52–58. [[CrossRef](#)]
40. Engelhart, M.J.; Geerlings, M.I.; Ruitenberg, A.; van Swieten, J.C.; Hofman, A.; Wittman, J.C.; Breteler, M.M. Dietary intake of antioxidants and risk of Alzheimer disease. *JAMA* **2002**, *287*, 3223–3229. [[CrossRef](#)]
41. Baloyannis, S.J. Mitochondrial alterations in Alzheimer's disease. *J. Alzheimer's Dis.* **2006**, *9*, 119–126. [[CrossRef](#)] [[PubMed](#)]
42. Wisniewski, H.M.; Wegiel, J. Beta-amyloid formation by myocytes of leptomeningeal vessels. *Acta Neuropathol.* **1994**, *87*, 233–241. [[CrossRef](#)] [[PubMed](#)]
43. Calhoun, M.E.; Burgermeister, P.; Phinney, A.L.; Stalder, M.; Tolnay, M.; Wiederhold, K.H.; Abramowski, D.; Sturchler-Pierrat, C.; Sommer, B.; Staufenbiel, M.; et al. Neuronal overexpression of mutant amyloid precursor protein results in prominent deposition of cerebrovascular amyloid. *Proc. Natl. Acad. Sci. USA* **1999**, *96*, 14088–14093. [[CrossRef](#)] [[PubMed](#)]
44. Herzig, M.C.; Winkler, D.T.; Burgermeister, P.; Pfeifer, M.; Kohler, E.; Schmidt, S.D.; Danner, S.; Abramowski, D.; Sturchler-Pierrat, C.; Bürki, K.; et al. A β is targeted to the vasculature in a mouse model of hereditary cerebral hemorrhage with amyloidosis. *Nat. Neurosci.* **2004**, *7*, 954–960. [[CrossRef](#)] [[PubMed](#)]
45. Yamagishi, S.I.; Edelstein, D.; Du, X.L.; Kaneda, Y.; Guzmán, M.; Brownlee, M. Leptin induces mitochondrial superoxide production and monocyte chemoattractant protein-1 expression in aortic endothelial cells by increasing fatty acid oxidation via protein kinase A. *J. Biol. Chem.* **2001**, *276*, 25096–25100. [[CrossRef](#)] [[PubMed](#)]
46. Cardenes, N.; Corey, C.; Geary, L.; Jain, S.; Zharikov, S.; Barge, S.; Novelli, E.M.; Shiva, S. Platelet bioenergetic screen in sickle cell patients reveals mitochondrial complex V inhibition, which contributes to platelet activation. *Blood* **2014**, *123*, 2864–2872. [[CrossRef](#)]
47. Hottz, E.D.; Oliveira, M.F.; Nunes, P.C.; Nogueira, R.M.; Valls-de-Souza, R.; Da Poian, A.T.; Weyrich, A.S.; Zimmerman, G.A.; Bozza, P.T.; Bozza, F.A. Dengue induces platelet activation, mitochondrial dysfunction and cell death through mechanisms that involve DC-SIGN and caspases. *J. Thromb. Haemost.* **2013**, *11*, 951–962. [[CrossRef](#)]

-
48. Puskarich, M.A.; Cornelius, D.C.; Tharp, J.; Nandi, U.; Jones, A.E. Plasma syndecan-1 levels identify a cohort of patients with severe sepsis at high risk for intubation after large-volume intravenous fluid resuscitation. *J. Crit. Care* **2016**, *36*, 125–129. [[CrossRef](#)]
 49. Lust, W.D.; Taylor, C.; Pundik, S.; Selman, W.R.; Ratcheson, R.A. Ischemic cell death: Dynamics of delayed secondary energy failure during reperfusion following focal ischemia. *Metab. Brain Dis.* **2002**, *17*, 113–121. [[CrossRef](#)]
 50. Kalogeris, T.; Bao, Y.; Korthuis, R.J. Mitochondrial reactive oxygen species: A double edged sword in ischemia/reperfusion vs preconditioning. *Redox Biol.* **2014**, *2*, 702–714. [[CrossRef](#)]